Polym. Bull. (2010) 64:791–804
DOI 10.1007/s00289-009-0214-0

ORIGINAL PAPER

# A thermosensitive chitosan/poly(vinyl alcohol) hydrogel containing nanoparticles for drug delivery

**Yufeng Tang · Yiyang Zhao · Yan Li · Yumin Du**

Received: 2 April 2009 / Revised: 17 November 2009 / Accepted: 21 November 2009 /
Published online: 3 December 2009


**Abstract** The synthesis and characterization of a thermosensitive chitosan (CS)/poly(vinyl alcohol) (PVA) hydrogel containing nanoparticles with different charges for drug delivery were reported. Through the electrostatic effect of $-N^+(CH_3)_3$ and $-COO^-$, the nanoparticles of *N*-(2-hydroxyl) propyl-3-trimethyl ammonium chitosan chloride(HTCC)–carboxymethyl chitosan (CM) were prepared. The nanoparticles with different charges were obtained by the different ratio of $-N^+(CH_3)_3$ and $-COO^-$, which were suitable for drug delivery with opposite charges, such as propranolol and diclofenac sodium, respectively. The release of the positive drug was the slowest with the hydrogels containing negative nanoparticles. Similarly, the release of the negative drug was the slowest with the hydrogels containing positive nanoparticles. However, the releases of the two drugs were both the fastest with the pure hydrogels. It indicated the addition of nanoparticles was helpful to slow the suitable drug release. Though the nanoparticles did not reinforce the gel strength, the electrostatic effect between nanoparticles and drugs reduced the burst release. Therefore, the composite gels are attractive for applications as carriers for drug delivery.

**Keywords** Nanocomposites · Hydrogels · Drug delivery

Y. Tang · Y. Li · Y. Du (✉)
College of Resource and Environmental Science, Wuhan University, Wuhan 430072, China
e-mail: duyumin@whu.edu.cn

Y. Tang · Y. Zhao
College of Chemistry and Pharmaceutical Engineer, NanYang Normal University,
NanYang 473061, China

## Introduction

Chitosan (CS), a polysaccharide derived from naturally abundant chitin, is currently receiving a great deal of interest for biomedical application because of good biocompatibility, biodegradability, and bioactivities [1]. The CS-based thermosensitive hydrogel systems have been extensively studied for biomedical applications, e.g. drug delivery [2, 3] and tissue engineering [4, 5]. All of them are injectable liquid at low temperature and transform to semisolid hydrogels at body temperature. It is mainly because that the temperature responsive hydrogels do not require organic solvents, copolymerization agents, or externally applied trigger for gelation suitable for biomaterial applications [6].

Chenite et al. [7] first developed a novel approach to produce thermosensitive neutral hydrogel based on CS/polyol salt combinations that could undergo sol–gel transition at a temperature close to 37 °C. Other researchers also evaluated the hydrogel for use in pharmaceutical applications [8, 9] and cartilage repair [10]. Many modified CS polymers also have thermosensitive characteristics, such as the PEG-grafted CS [11], hydroxybutyl CS [12], *N*-isopropylacrylamide-grafted CS [13] and quaternized CS [14]. All of them are injectable liquid at low temperature and transform to semisolid hydrogels at body temperature. Therefore, they have a broad range of medical applications, particularly for sustained in vivo drug release and tissue engineering. However, the burst delivery of drug-loaded gels is obvious. This disadvantage can restrict their applications as biomaterials.

Nanoparticles have been proposed as drug delivery systems with potential applications such as prolonging the residence time of drugs in the blood circulation [15] or improving transmucosal transport of macromolecular bioactive compounds [16]. In recent years, nanoparticles based on polyelectrolyte complexes from oppositely charged macromolecules as controlled drug release formulations, especially for peptide and protein drug delivery, have attracted considerable attention [17–20]. Polyelectrolytes are macromolecules carrying a relatively large number of functional groups that either are charged, or under suitable conditions, can become charged [21]. The macromolecules may constitute either polycations or polyanions, depending on their functional group type. Polyelectrolyte complexes are therefore formed by the reaction of one polyelectrolyte with another oppositely charged polyelectrolyte in an aqueous solution. The process is simple, feasible, and usually performed under mild conditions. Another advantage of this system is that since preparation of the complex is through physical crosslinking by electrostatic interactions instead of chemical crosslinking; the possibility of toxicity associated with crosslinking reagents involved in chemical crosslinking processes can be eliminated. Among these polymers, polysaccharides have been frequently studied for drug delivery and medical applications. A few papers [22–24] also reported the quaternized chitosan nanoparticles were biocompatible and non-toxic according to cytotoxicity assay and used as antibacterial agent, drug, and gene delivery system. Through the electrostatic effect of $-N^{+}(CH_3)_3$ and $-COO^{-}$, the nanoparticles of *N*-(2-hydroxyl) propyl-3-trimethyl ammonium chitosan chloride (HTCC)–carboxymethyl chitosan (CMCS) were prepared. The nanoparticles with different charges were obtained by

the different ratio of $-N^{+}(CH_3)_3$ and $-COO^{-}$, which were suitable for drug delivery with opposite charges, such as propranolol and diclofenac sodium.

In our previous study, the thermosensitive CS/poly(vinyl alcohol) (PVA) blend hydrogel for drug delivery was investigated [25]. It was found that the drug burst was severe. In order to slow the drug release, the thermosensitive CS/PVA hydrogel containing different charged nanoparticles for drug delivery was first synthesized. The results showed the electrostatic effect between nanoparticles and drugs reduced the burst release. Therefore, the composite gels are promising to be used as injectable in situ forming systems for drug delivery and tissue engineering.

## Experimental

### Materials

Chitosan was obtained from Yuhuan Ocean Biochemistry Co. (Zhejiang, China). The deacetylation degree (DD) as determined by elemental analysis was 92%, and the molecular weight calculated from the GPC method was about $2.7 \times 10^5$. Standard pullulans for GPC were purchased from Showa Denko, Tokyo, Japan. PVA with an average degree of polymerization of 2400–2500 were purchased from Shanghai Chemical Reagent Co. (Shanghai, China). All other chemicals were of analytical grade.

### Preparation of CMCS

Carboxymethyl chitosan were prepared based on our previous work [26, 27]. In brief, 10 g CS were frozen at −20 °C in 10 mL alkali solution(50 wt%) for 12 h, then transferred to 100 mL 2-propanol, and 12.0 g $ClCH_2COOH$ was added in portions. The mixture was kept stirring at 20 °C for 2 h then for another 4 h at 60 °C. After dialyzing and vacuum dried, N, O–CMCS was obtained. DS values of prepared products were estimated from potentiometric titration as 0.63. Molecular weights of the prepared CMCS were measured by gel-permeation chromatography (GPC), as 22.8 kDa.

### Preparation of HTCC

Quaternary CS was prepared based on our previous work [17]. Briefly, epoxy chloropropane was added to the mixture of concentrated hydrochloric acid and trimethylamine under stirring, then aqueous NaOH equivalent to amount of hydrochloric acid was dropped in slowly to obtain 2,3-epoxypropyltrimethyl ammonium chloride (EPTMAC), EPTMAC was refined by vacuum distillation and extracted with ether. CS (10 g) was dispersed in distilled water and EPTMAC was added, the reaction mixture was then adjusted to pH 9. After 8 h of stirring at 80 °C, the CS particles were completely dissolved in water. After dialyzed against distilled water for 4 days, the solution was precipitated with acetone to get HTCC, which was then

dried overnight in vacuo for further use. Mws of HTCC were measured to be 230 kDa by GPC analysis connected with a refractive index detector. DS was determined by potentiometry to be 0.61.

## Preparation, morphology, and structure characterization of the nanoparticles in deionized water

1.0–2.5 mg HTCC and 1.0–2.5 mg CMCS were dissolved in the deionized water (10 mL), respectively. Then, they were mixed in the different concentration to obtain nanoparticles in the different $n^+/n^-$.

FTIR spectra were recorded on an FTIR spectrometer (Nicolet, Model Impact 410, WI) at room temperature. HTCC, CMCS, and the dried HTCC/CMCS nanoparticles were triturated with KBr in the ratio of 1:100 and pressed to form a pallet. All the samples were scanned from 400–4,000 cm.

TEM (100 CX II, Japan) was used to observe the morphology of the HTCC/CMCS nanoparticles. Samples were placed onto copper grill and dried at room temperature, then examined without being stained.

The mean size and size distribution of the HTCC/CMCS nanoparticles were measured by dynamic light scattering (DLS) (Zetasize; 3000 HS, Malvern, UK). All measurements were done with a wavelength of 633.0 nm at 25 °C with an angle detection of 90°.

## Preparation of HTCC/CMCS-CS/PVA composite gels

A clear solution of CS was obtained by dissolving 200 mg of CS in 10 mL of HCl solution (0.1 M) and chilled in an ice bath for 15 min, which was containing 1–2.5 mg HTCC. PVA was added to deionized water and heated at 80 °C for 1 h to make a solution containing 2 wt% PVA by weight. The solution of $NaHCO_3$ (1 mL, 1.0 M) and PVA (10 mL, 2 wt%) were mixed and chilled for 15 min similarly, which was containing 1–2.5 mg CMCS. Then, the latter was slowly added to the former in an ice bath under magnetic stirring for 10 min. The solution was degassed by centrifugation of samples at 5000*g* and 5 °C for 5 min. The gel was formed in half hour at 37 °C.

## Rheological measurement

The rheological properties were performed on a strain-controlled ARES rheometer (TA Inc., New Castle, USA). The rheometer was equipped with two sensitive force transducers fro torque measurements ranging from 0.004 to 100 g cm. A Couette (two concentric cylinders) cell geometry was used for monitoring the steady-state shear flow and dynamic rheology of the samples modulus. The rheometer is equipped with a thermo-bath with circulating water that was calibrated to give a temperature in the sample chamber within ±0.5 °C of the set value. The degassed solution of 10 mL was heated or cooled to desired temperature directly in the rheometer (without shearing or oscillating) and then covered with mineral oil to

prevent evaporation during the measurements. For the frequency and time sweep measurements, it was defined as time $t = 0$ s when the temperature reaches the desired temperature. The sweep of the frequency was from 0.1 to 200 rad/s, and each frequency sweep took 900 s to be completed.

### Drug load and release

After a model drug was dissolved in PVA solution, the drug-loaded hydrogels were fabricated following the same procedure as described in the preparation of HTCC/CMCS–CS/PVA hydrogel. The drug-loaded hydrogels were immersed in 20 mL of 0.1 M pH 7.4 phosphate buffered saline (PBS) in a conical flask and incubated at 37 °C in a thermostated shaker rotating at 100 rpm. Then 5 mL of this solution was taken out at regular intervals, and the release of drug was estimated at 290 nm by using UV spectrophotometer. With each sampling, the solution was changed with fresh medium, maintaining the total volume constant. The percentage of cumulative amount of released drug was determined from standard calibration curves. The blank hydrogel was measured at the same way to reduce the effect of chitosan.

## Results and discussion

### Formation of nanoparticles

Through the electrostatic effect of $-N^+(CH_3)_3$ and $-COO^-$, the HTCC/CMCS nanoparticles were prepared. The different ratio of $-N^+(CH_3)_3$ and $-COO^-$ had an important effect on the formation and stabilization of nanoparticles. Figure 1 showed the stabilities of HTCC/CM nanoparticles at different charges and concentrations by turbidity analysis. When the charge ratio of $n^+/n^-$ was equal to 1, the stabilities of nanoparticles was the lowest. As the zeta charge was about close to 0, the conglomerations were easy to be formed and the solution became clear after the conglomerations were deposited. The closer the charge ratio of $n^+/n^-$ was to 1, such as 0.8 and 1.25, the lower the stabilities of nanoparticles. The nanoparticles had happened to different extent of flocculation after 1 day. On the contrary, the stronger zeta charge of nanoparticles the higher the stabilities. When the concentration of nanoparticles was increased, the stabilities were reduced because of the conglomerations.

### Characterization of nanoparticles

Figure 2 showed the morphological characteristic of nanoparticles with the different charge ratio. When the charge ratio of $n^+/n^-$ was equal to 1.67 (Fig. 2a), the nanoparticles had good spherical shape and monodisperse. When the charge ratio of $n^+/n^-$ was equal to 1.25 (Fig. 2b), the nanoparticles had slightly aggregated. When $n^+/n^-$ was equal to 1 (Fig. 2c), many aggregates had been formed and the particles had larger sizes. It meant the charge played important roles in formation and

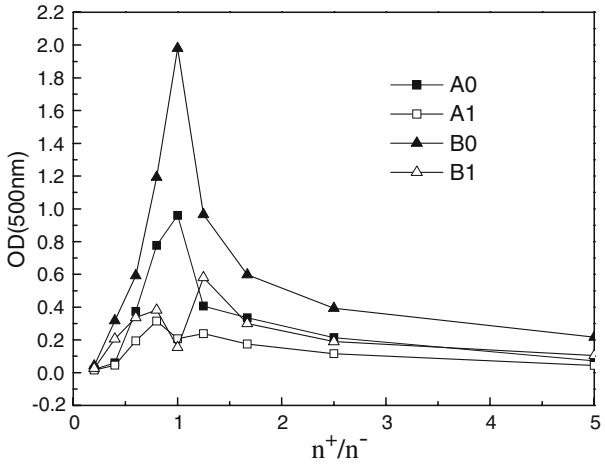


**Fig. 1** Stabilities of HTCC/CMCS nanoparticles at different charges and concentrations (A: high concentrations; B: low concentrations; 0:1 h; 1:1d)

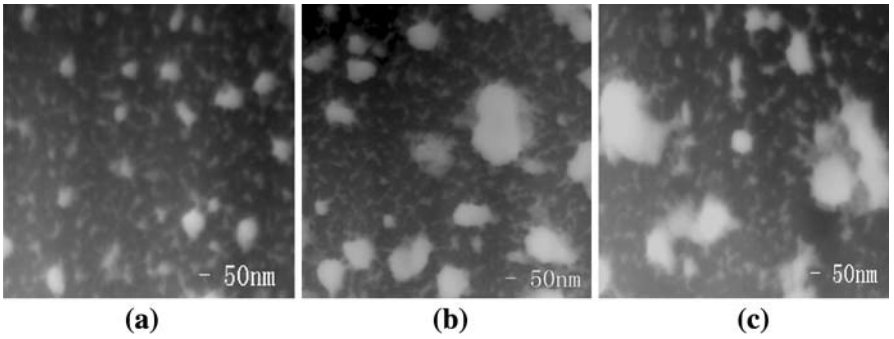


**Fig. 2** TEM of HTCC/CMCS nanoparticles ($n^+/n^-$, **a** = 1.67; **b** = 1.25; **c** = 1)

**Table 1** Sizes and charges of HTCC/CMCS nanoparticle

| Samples | HTCC concentration (mg/mL) | CMCS concentration (mg/mL) | Particles sizes (nm) | Particle charges |
|---|---|---|---|---|
| 1 | 0.25 | 0.15 | 246.9 | 32.05 |
| 2 | 0.25 | 0.2 | 254.5 | 21.1 |
| 3 | 0.15 | 0.25 | 273.4 | −21.8 |
| 4 | 0.2 | 0.25 | 294.7 | −16.31 |

attribution of nanoparticles. The $n^+/n^-$ ratio 1.67, 1.25, and 1 meant the ζ-potential values 32.05, +21.1, 0 mV, respectively. With the decrease of the $n^+/n^-$ ratio, the absolute ζ-potential values reduced, and the aggregates were easier to appear.

Table 1 also showed the sizes and ζ-potential of nanoparticles. All nanoparticles showed the size in the range of 200–300 nm. It was found that the particle size was

evidently affected by the ζ-potential values. The ζ-potential values of the positive particles were +32.05 and +21.1 mV, respectively. The ζ-potential values of the negative particles were −21.8 and −16.31 mV, respectively. The ζ-potentials of the HTCC/CMCS particles appear positive values which were higher than that of negative nanoparticles. Specially, with the increase of the absolute ζ-potential values, the sizes of nanoparticles were smaller. The result indicated the nanoparticles dispersed uniformly had the smallest sizes because of the highest absolute ζ-potential value. ζ-potential of the nanoparticles can greatly influence their stability in suspension through electrostatic repulsion between the particles.

## FTIR analysis

The IR spectra of HTCC (A), CMCS (B), and HTCC/CMCS (C) nanoparticles were presented in Fig. 3. In the spectrum A, the broad peak at 3400–3200 $cm^{-1}$ is caused by O–H and N–H stretching vibration. Peak at 2900 $cm^{-1}$ is due to the C–H stretching vibrations. The sharp peak at 1480 $cm^{-1}$ is attributed to the methyl groups of the ammonium. In the spectrum B, the absorption bands at 1,600 and 1,420 $cm^{-1}$ are due to the asymmetrical and symmetrical $–COO^-$ stretching vibration. The spectra of C showed a decrease in intensity of the $–COO^-$ group absorption band. The intensity of 1480 $cm^{-1}$ peak becomes weaker. It evidenced the electrostatic interaction between amino group of HTCC and carboxyl group of CMCS. The broad band at 3,400–3,200 $cm^{-1}$ was little change in the shape and wavenumber in HTCC–CMCS and nanoparticles, which suggested that neither the –OH nor the $–NH_2$ group are involved in the coordination of $–NH_3^+$ and $–COO^-$.

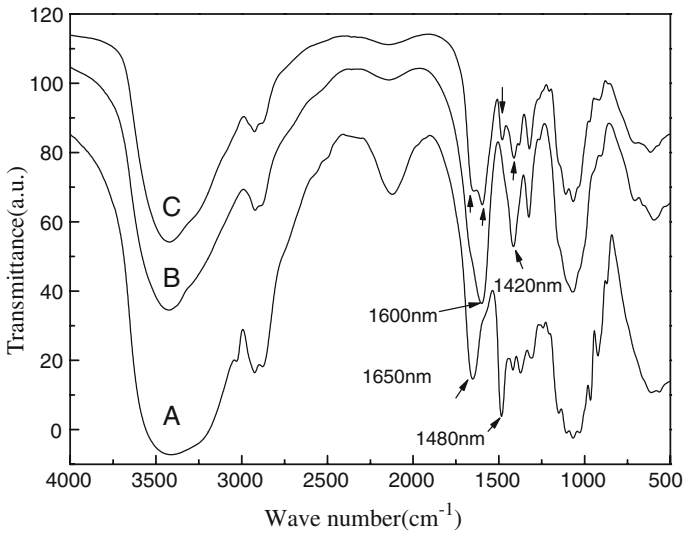


**Fig. 3** FTIR spectra of HTCC (A), CMCS (B), and HTCC/CMCS nanoparticles (C)

## Rheological analysis

The dynamic mechanical characterization is useful for understanding the formation mechanism of the hydrogels and consequently their possible applications. In our previous study [25], the formation mechanism of pure CS/PVA gel had been discussed. The hydrophobic interactions are assumed to be the main driving force to form the gel consisting of CS and PVA at high temperature. For HTCC/CMCS-CS/PVA composite gels, different charges of HTCC/CMCS nanoparticles were formed among the CS/PVA gel. The effect of nanoparticles on gel formation was further studied by rheological analysis.

### *Gel frequency*

The frequency dependence of the viscoelastic properties of composites was revealed at different temperatures in Fig. 4. For each sample, the G′ and G″ are measured as a function of the frequency from 0.1 to 100 Hz. The data are shifted along vertical axes by $10^a$ with given $a$ value to avoid overlapping.

The different viscoelastic properties of three hydrogels at different temperatures might be attributed to the different gelation temperatures. When the ambient temperature is largely lower than the gel temperature, the loss modulus G″ is higher than the storage modulus G′ within the frequency range. Those features are characteristic of the stable viscous liquid. With an increase of the temperature close to the gel temperature, the difference between G′ and G″ becomes small, that is close to gelation. Furthermore, when the ambient temperature is equal to and even slightly higher than the gel temperature, G′ is gradually increased to exceed G″. It means the gel has been formed. However, the further increase in frequency causes a significant decrease in storage modulus, which is indicative of structure break by mechanical shear. The storage modulus becomes lower than the loss modulus, and the system behaves like a solution. Their rheological behavior is typical of a "weak gel," which has the frequency dependence. At last, when the ambient temperature is obviously higher than the gel temperature, G′ is always higher than G″ over the whole frequency range. It is evident that the storage modulus G′ shows almost no dependence with frequency. These features are characteristic of a "strong gel."

Therefore, the gelation temperature of pure CS/PVA gel (A) was about 20 °C. The gel temperature of HTCC/CMCS-CS/PVA composite gels was improved. Especially for the gels containing negative nanoparticles, the gel temperature was 30 °C. It indicated the nanoparticles had effect on gel formation. For the gels containing nanoparticles, the reaction between $NH_3^+$ of CS and $HCO_3^-$ was influenced because different charges. The hydrophobic interactions of CS chains were reduced, and the gel temperature was improved. The positive nanoparticles had the interaction with $HCO_3^-$. It resulted that the less $NH_3^+$ was changed to $NH_2$. Therefore, the hydrophobic interactions of CS chains were reduced, and the gel temperature was improved. The negative nanoparticles had the interaction with $NH_3^+$. The reaction of $HCO_3^-$ and $NH_3^+$ was reduced, and pH value was lower than the pure CS/PVA gel. This also resulted in the decrease of hydrophobic interactions of CS chains and the elevation of the gel temperature.

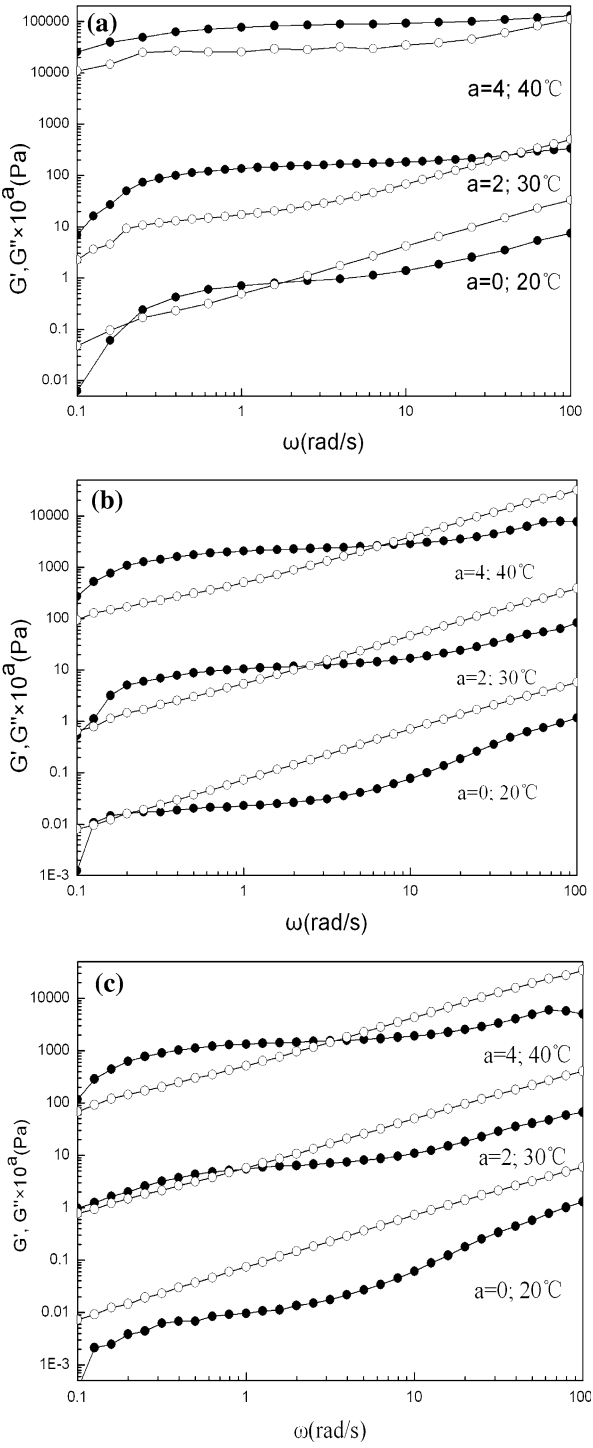


**Fig. 4** Frequency dependence of G′ and G″ of gels at different temperature. Closed and open symbols denote G′ and G″, respectively. The data are shifted along vertical axes by $10^a$ with given a value to avoid overlapping. **a** Pure CS/PVA gel; **b** HTCC/CMCS-CS/PVA gels; (HTCC: 0.25 mg/mL; CMCS: 0.15 mg/mL); **c** HTCC/CMCS-CS/PVA gels. (HTCC: 0.15 mg/mL; CMCS: 0.25 mg/mL)

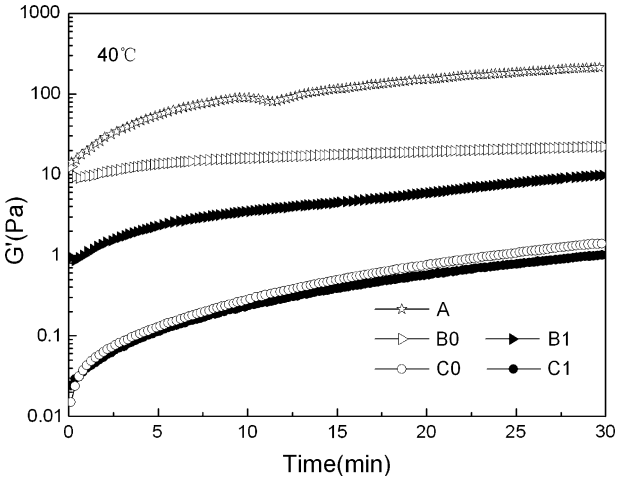


**Fig. 5** Time dependence of storage modulus G′ at 40 °C. A: pure CS/PVA gel; B: HTCC/CMCS-CS/PVA gels; (B0: HTCC (0.5 mg/mL)/CMCS (0.3 mg/mL); B1: HTCC (0.25 mg/mL)/CMCS (0.15 mg/mL)); C: HTCC/CMCS-CS/PVA gels. (C0: HTCC (0.3 mg/mL)/CMCS (0.5 mg/mL); C1: HTCC(0.15 mg/mL)/CMCS (0.25 mg/mL))

### *Gel strength*

As known, the storage modulus can be considered as a measure of the extent of gel network formation. The higher G′ value of the gel means the stronger gel intensity. Therefore, as shown in Fig. 5, the charge and concentration of nanoparticles had a great effect on gel strength at the same temperature. For example, the storage modulus G′ of A, B, and C was 210, 25, and 1 Pa at 40 °C at 1 Hz, respectively. It meant the gel strength was notably decreased by the particles, especially negative nanoparticles.

## Drug delivery

### *Effect of different charge drug*

With propranolol as a positive model drug and diclofenac sodium as negative model drug, cumulative releases of drug with the composite gels were shown in Fig. 6. As the two drugs had no interaction with the pure CS/PVA gel, the release profiles exhibited a burst release in the first 1 h from the pore of gel. Further, the collapse of gel scaffold made the drugs completely release over 24 h. However, the release of the negative drug was the slowest when the hydrogels containing positive nanoparticles were used as drug carrier (Fig. 6a). It meant the positive nanoparticles captured the negative drug inside the gels, and this could restrict the delivery. Similarly, the release of the positive drug was the slowest with the hydrogels

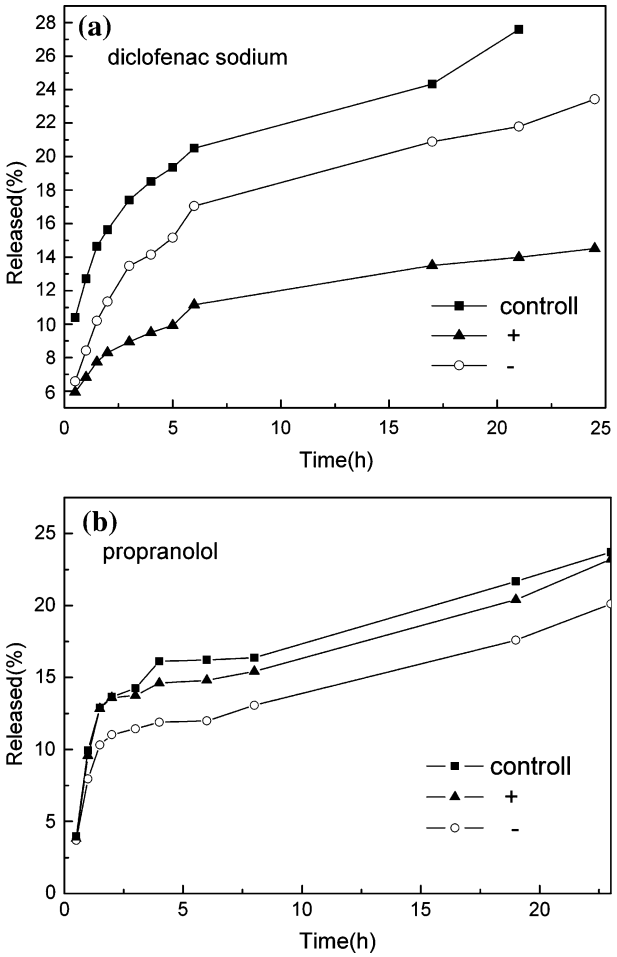


**Fig. 6** Drug delivery of CS/PVA gels with different charges drugs

containing negative nanoparticles even if the nanoparticles didn't reinforce the gel strength (Fig. 6b).

*Effect of different charge nanoparticles*

Figure 7 showed the delivery of diclofenac sodium with the hydrogels containing different positive nanoparticles. When the charge ratio of $n^+/n^-$ was equal to 1.67, the nanoparticles had good spherical shape and monodisperse. Therefore, the drug release was the slowest. Figure 8 showed the delivery of propranolo with the hydrogels containing different negative nanoparticles. As the gel strength containing negative nanoparticles was reduced according to the rheological analysis, the different charge of negative nanoparticles had no important effect on drug releases.

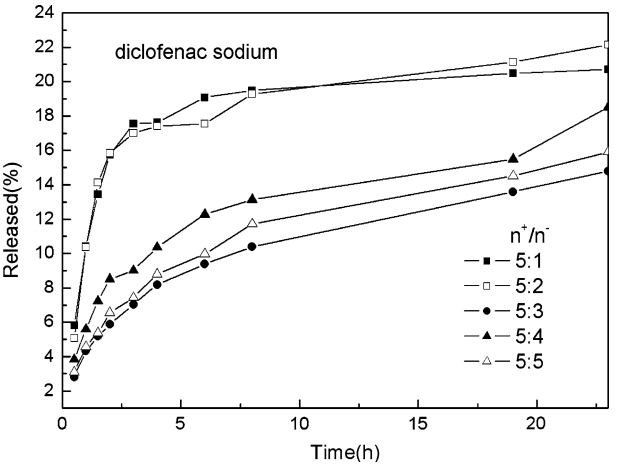


**Fig. 7** Drug delivery of CS/PVA gels with different charges nanoparticles

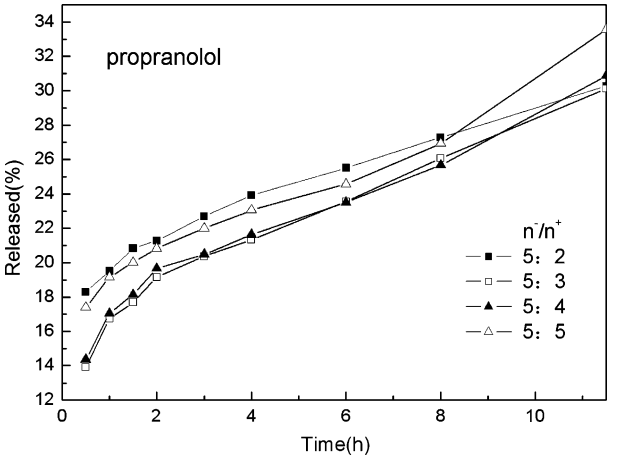


**Fig. 8** Drug delivery of CS/PVA gels with different charges nanoparticles

## Conclusions

The novel composite gels containing different charge nanoparticles with complicated porous structure were firstly synthesized. The electrostatic interaction of $-N^{+}(CH_3)_3$ and –COO– was the major factor on the formation of nanoparticles. They had good spherical shape and monodisperse (sizes, 200–300 nm) at the appropriate charge ratio of $n^{+}/n^{-}$ through the observation of FTIR, DLS, and TEM. When the nanoparticles were formed inside the hydrogel, the composites were liquid aqueous solutions at low temperature (about 4 °C), but gels under physiological conditions. The rheological analysis indicated that the gel strength was reduced by the formation of particles, especially negative nanoparticles.

However, the electrostatic effect between nanoparticles and drugs reduced the burst release. Therefore, the novel HTCC/CM–CS/PVA composite gels are attractive for applications as drug delivery, artificial bones and scaffolds for tissue engineering.

**Acknowledgment** The work was supported in part by the Special Foundation of Nanyang Normal University (No. 200752 and 200751) and the National Natural Science Foundation of China (No: 30770574).

## References

1. Rinaudo M (2006) Chitin and chitosan: properties and applications. Prog Polym Sci 31:603–632
2. Hsiue GH, Chang RW, Wang CH, Lee SH (2003) Development of in situ thermosensitive drug vehicles for glaucoma therapy. Biomaterials 24:2423–2430
3. Gariepy ER, Chenite A, Chaput C, Guirguis S, Leroux JC (2000) Characterization of thermosensitive chitosan gels for the sustained delivery of drugs. Int J Pharm 203:89–98
4. Shu XZ, Liu YC, Palumbo FS, Luo Y, Prestwich GD (2004) In situ crosslinkable hyaluronan hydrogels for tissue engineering. Biomaterials 25:1339–1348
5. Anseth KS, Metters AT, Bryant SJ, Martens PJ, Elisseeff JH, Bowman CN (2002) In situ forming degradable networks and their application in tissue engineering and drug delivery. J Control Release 78:199–209
6. Jeong B, Kim SW, Baeb YH (2002) Thermosensitive sol–gel reversible hydrogels. Adv Drug Deliv Rev 54:37–51
7. Chenite A, Chaput C, Wang D, Combes C, Buschmann MD, Hoemann CD, Leroux JC, Atkinson BL, Binette F, Selmani A (2000) Novel injectable neutral solutions of chitosan form biodegradable gels in situ. Biomaterials 21:2155–2161
8. Gariepy ER, Leclair G, Hildgen P, Gupta A, Leroux JC (2002) Thermosensitive chitosan-based hydrogel containing liposomes for the delivery of hydrophilic molecules. J Control Release 82:373–383
9. Ruel-Gariepy E, Leroux JC (2004) In situ-forming hydrogels—review of temperature-sensitive systems. Eur J Pharm Biopharm 58:409–426
10. Hoemann CD, Sun J, Legare A, McKee MD, Ranger P, Buschmann MD (2001) A thermosensitive polysaccharide gel for cell delivery in cartilage repair. Trans Orthop Res Soc 26:626
11. Bhattarai N, Ramay HR, Gunn J, Matsen FA, Zhang MQ (2005) PEG-grafted chitosan as an injectable thermosensitive hydrogel for sustained protein release. J Control Release 103:609–624
12. Dang JM, Sun DN, Ya YS, Sieber AN, Kostuik JP, Leong KW (2006) Temperature-responsive hydroxybutyl chitosan for the culture of mesenchymal stem cells and intervertebral disk cells. Biomaterials 27:406–418
13. Chung HJ, Bae JW, Park HD, Lee JW, Park KD (2005) Thermosensitive chitosans as novel injectable biomaterials. Macromol Symp 224:275–286
14. Wu J, Su ZG, Ma GH (2006) A thermo- and pH-sensitive hydrogel composed of quaternized chitosan/glycerophosphate. Int J Pharm 315:1–11
15. Gref R, Minamitake Y, Peracchia MT, Trubetskoy V (1994) Biodegradable long-circulating polymeric nanospheres. Science 263:1600–1603
16. Mathiowitz E, Jacob JS, Jong YS, Carino GP, Chickering DE, Chaturvedi P, Santos CA, Vijayaraghavan K, Montgomery S, Bassett M, Morrel C (1997) Biologically erodable microspheres as potential oral drug delivery systems. Nature 386:410–414
17. Xu YM, Du YM, Huang RH, Gao LP (2003) Preparation and modification of N-(2-hydroxyl)propyl-3-trimethyl ammonium chitosan chloride nanoparticle as a protein carrier. Biomaterials 24:5015–5022
18. Shi XW, Du YM, Sun LP, Yang JH, Wang XH, Su XL (2005) Ionically crosslinked alginate/carboxymethyl chitin beads for oral delivery of protein drugs. Macromol Biosci 5:881–889
19. Chen Q, Hu Y, Chen Y, Jiang XQ, Yang YH (2005) Microstructure formation and property of chitosan-poly(acrylic acid) nanoparticles prepared by macromolecular complex. Macromol Biosci 5:993–1000

20. Hu Y, Jiang XQ, Ding Y, Ge HX, Yuan YY, Yang CZ (2002) Synthesis and characterization of chitosan-poly(acrylic acid) nanoparticles. Biomaterials 23:3193–3201
21. Spalla O (2002) Nanoparticle interactions with polymers and polyelectrolytes. Curr Opin Colloid Int Sci 7:179–185
22. Shi ZL, Neoha KG, Kanga ET, Wang W (2006) Antibacterial and mechanical properties of bone cement impregnated with chitosan nanoparticles. Biomaterials 27:2440–2449
23. Wang XY, Du YM, Luo JW (2008) Biopolymer/montmorillonite nanocomposite: preparation, drug-controlled release property and cytotoxicity. Nanotechnology 19(6): 65707-1-65707-7
24. Wang XY, Pei XF, Du YM, Li Y (2008) Quaternized chitosan/rectorite intercalative materials for a gene delivery system. Nanotechnology 19:375102
25. Tang YF, Du YM, Hu XW, Shi XW, Kennedy JF (2007) Rheological characterisation of a novel thermosensitive chitosan/poly(vinyl alcohol) blend hydrogel. Carbohydr Polym 67:491–499
26. Chen LY, Tian ZG, Du YM (2004) Synthesis and pH sensitivity of carboxymethyl chitosan-based polyampholyte hydrogels for protein carrier matrices. Biomaterials 25:3725–3732
27. Sun LP, Du YM, Yang JH, Shi XW, Li J, Wang XH, Kennedy JF (2006) Conversion of crystal structure of the chitin to facilitate preparation of a 6-carboxychitin with moisture absorption-retention abilities. Carbohyd Polym 66:168–175